THE JOURNAL OF PHYSICAL CHEMISTRY C

Article

pubs.acs.org/JPCC

Host–Guest Superstructures on Graphene-Based Kagome Lattice

Haigang Zhang, W.D. Xiao, Jinhai Mao, Haitao Zhou, Geng Li, Yi Zhang, Liwei Liu, Shixuan Du, and H.-J. Gao*

Beijing National Laboratory of Condensed Matter Physics, Institute of Physics, Chinese Academy of Sciences, Beijing 100190, P. R. China

Supporting Information

ABSTRACT: The Kagome lattice of iron phthalocyanine (FePc) on the graphene moiré pattern is employed as host template for two kinds of guest molecules, FePc and *tert*-butyl zinc phthalocyanine ((*t*-Bu)$_4$–ZnPc), to fabricate stable host–guest molecular superstructures. Both FePc and (*t*-Bu)$_4$–ZnPc molecules prefer to occupy the nanoscale pores of the Kagome lattice. Ordered superstructures with alternate rows of FePc and (*t*-Bu)$_4$–ZnPc are formed after coadsorption of these two species with a ratio of 1:1 on the Kagome lattice. We elucidate that formation of ordered superstructures of guest FePc and (*t*-Bu)$_4$–ZnPc are controlled by long-range interaction between the guest molecules mediated by the host Kagome lattice with additional contribution from the graphene/Ru(0001) substrate.

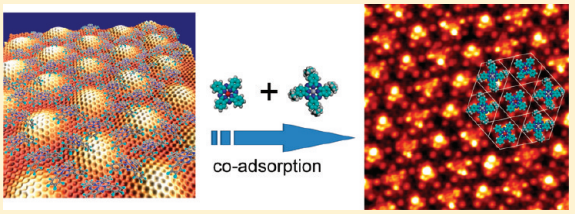

INTRODUCTION

Constructing highly ordered multicomponent supramolecular structures on solid surfaces has been attracting considerable attention for potential applications in molecular devices.[1−8] In recent years a variety of two-dimensional (2D) porous networks have been fabricated through directional and selective noncovalent intermolecular interactions,[1−8] e.g., hydrogen bonding,[9−12] metal coordination,[13] and dipolar coupling.[14] Accommodation of additional guest molecules in the cavities of the open networks has been demonstrated.[9,13,15−25] However, such 2D open networks are usually prepared on metal surfaces. Thus, the strong coupling between the molecules and the metal substrates might result in significant modifications of the intrinsic electronic and geometric structures of the molecules, hindering potential application of such supramolecular architectures.

As a 2D honeycomb lattice of sp^2-bonded carbon atoms, graphene has attracted great interest because of its novel properties and potential applications.[26−29] Recently, monolayer graphene (MG) has been epitaxially grown on various metal surfaces, e.g., Ru(0001),[30−33] Ir(111),[34] Pt(111),[35,36] Ni(111),[37,38] and Cu(111).[39] MG grown on metal surfaces can be used as a buffer layer to electronically decouple the adsorbed molecules from the substrates and preserve the intrinsic molecular electronic structures.[40−42] Moreover, adopting the moiré pattern of MG that originates from the lattice mismatch between MG and the Ru(0001) surface as a template,[30] regular Kagome lattices of metal phthalocyanines (MPc) molecules were fabricated.[43] The Kagome lattice, which is a 2D pattern composed of interlaced triangles whose lattice points have four neighboring points each,[44] duplicates the lattice of the moiré pattern of MG and provide regular arrays of nanoscale pores that might be used to host additional functional molecules.

In this work, we report on the accommodation of iron phthalocyanine (FePc) and *tert*-butyl zinc phthalocyanine ((*t*-Bu)$_4$–ZnPc) molecules by the porous Kagome lattice of FePc molecules on MG/Ru(0001). Scanning tunneling microscopy (STM) studies show that after deposition upon the host Kagome lattice each guest molecule of FePc or (*t*-Bu)$_4$–ZnPc prefers to occupy a nanoscale pore of the Kagome lattice at low coverage. With increasing coverage of guest molecules of either FePc or (*t*-Bu)$_4$–ZnPc alone the guest molecules condense into disordered aggregations. Ordered superstructures with alternate rows of FePc and (*t*-Bu)$_4$–ZnPc are formed after coadsorption of these two species with a ratio of 1:1 onto the Kagome lattice.

EXPERIMENTAL SECTION

Experiments were performed in an ultra-high-vacuum low-temperature STM system (Omicron) equipped with standard surface preparation facilities. The Ru(0001) surface was prepared by repeated cycles of sputtering with argon ions and annealing to 950 °C. High-quality and large-area MG was obtained via pyrolysis of ethylene on Ru(0001) substrate that was held at 950 °C.[30] The FePc, (*t*-Bu)$_4$–ZnPc, phthalocyanine (H_2Pc), and C_{60} molecules were deposited via vacuum sublimation from a Knudsen-type evaporator onto the sample that was kept at room temperature (RT). One monolayer (ML) refers to completion of a close-packed layer on Ru(0001), as estimated with STM. After vapor deposition of ~0.75 ML FePc upon MG at RT a regular molecular Kagome lattice is formed, as described in our previous report.[43] STM images were acquired in constant-current mode at a sample

Received: March 1, 2012
Revised: April 25, 2012
Published: April 26, 2012

   dx.doi.org/10.1021/jp3020244 | J. Phys. Chem. C 2012, 116, 11091−11095

temperature of ~5 K. The bias voltage was applied to the sample with respect to the tip.

RESULTS AND DISCUSSION

Clean MG grown on Ru(0001) exhibits a hexagonal moiré pattern composed of atop, fcc, and hcp regions with a periodicity of ~3 nm (Figure 1a) due to the lattice mismatch between MG and Ru(0001) surface.[30,33] After vapor deposition of ~0.75 ML FePc upon MG at RT a regular molecular Kagome lattice is formed,[43] as the FePc molecules preferentially occupy the fcc and hcp regions of the moiré pattern of MG on Ru(0001) (Figure 1b). The unoccupied atop regions of the moiré pattern constitute a hexagonal lattice that precisely duplicate the lattice constants of the moiré pattern of MG on Ru(0001), providing regular arrays of nanoscale pores for accommodation of guest molecules.

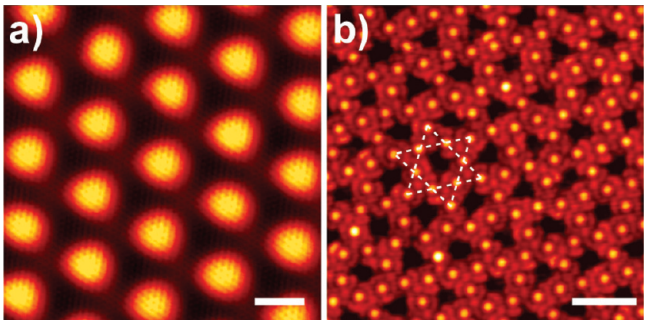

Figure 1. (a) STM image of the highly ordered moiré pattern of MG grown on Ru(0001) surface (scale bar = 2 nm). (b) Kagome lattice of FePc molecules fabricated on MG/Ru(0001) (scale bar = 4 nm). Dashed six-point star highlights the FePc Kagome lattice.

In order to investigate the hosting property of the porous Kagome lattice of FePc on MG/Ru(0001), guest FePc and (t-Bu)$_4$-ZnPc molecules were separately deposited on top of the Kagome lattice at RT. Figure 2a shows an STM image after addition of ~0.01 ML FePc molecules upon the prepared Kagome lattice of FePc on MG/Ru(0001). The most pronounced feature is a bright protrusion located at a pore site of the Kagome lattice. This pronounced protrusion is surrounded by four dim lobes. These features are consistent with the molecular structure of FePc,[43,45,46] thus assigned to a guest FePc molecule that is seated at the pore site of the Kagome lattice. The four dim lobes show rather similar apparent height, suggesting that the guest FePc molecule adopts a flat configuration with its molecular plane parallel to the surface.[43,45] Line profile analysis reveals that the apparent height of the central protrusion of the guest FePc molecule is ~0.23 nm higher than that of the FePc molecules constituting the host Kagome lattice, indicating that the molecular plane of the guest molecule is higher than that constituting the Kagome lattice. Each guest FePc molecule adopts a similar adsorption configuration with one of its high-symmetry axes rotated by ~38° with respect to a lattice vector of the Kagome lattice. We note that all guest FePc molecules are trapped at the pore sites of the Kagome lattice and no guest FePc molecule is adsorbed on top of individual FePc molecules constituting the Kagome lattice, demonstrating the capability of the porous Kagome lattice to accommodate guest molecules. The structural model of the host–guest supramolecular structures of FePc molecules on the Kagome lattice is shown in Figure 2c.

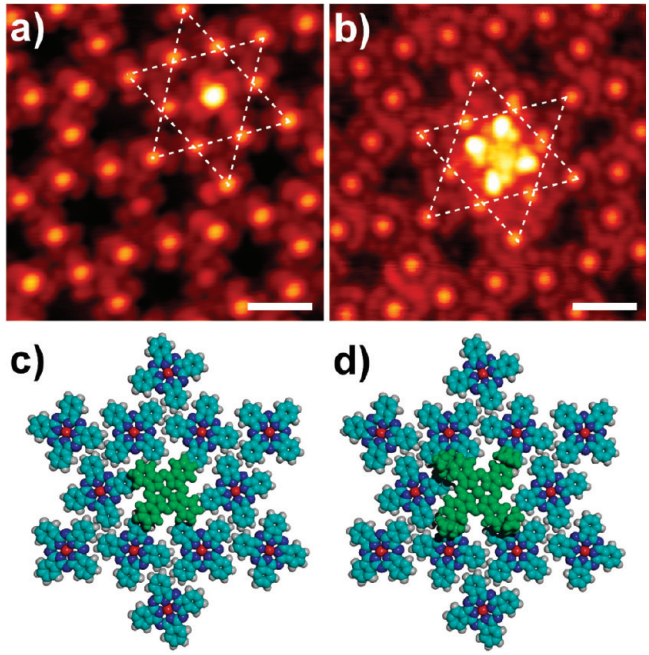

Figure 2. (a and b) STM images of single-guest FePc and (t-Bu)$_4$–ZnPc molecules hosted by FePc Kagome lattice, respectively (scale bar = 2 nm). Dashed six-point stars highlight the FePc Kagome lattice. (c and d) Schematics of guest FePc and (t-Bu)$_4$–ZnPc molecules on FePc Kagome lattice, respectively. Guest FePc and (t-Bu)$_4$–ZnPc molecules are colored in green to enhance the contrast to the surrounding FePc molecules of the host Kagome lattice.

A similar accommodation behavior is also observed for (t-Bu)$_4$–ZnPc molecules after separated sublimation of ~0.01 ML (t-Bu)$_4$–ZnPc molecules on top of a Kagome lattice of FePc molecules on MG/Ru(0001) at RT, as shown in Figure 2b. It is seen that the guest (t-Bu)$_4$–ZnPc molecule is seated at a pore site of the Kagome lattice and imaged as a cross with four bright lobes surrounding a dim center.[43,47] The four bright lobes show similar apparent heights, which are ~0.35 nm higher than the FePc molecules constituting the Kagome lattice, indicating that the (t-Bu)$_4$–ZnPc molecule also adopts a flat adsorption configuration with the molecular plane higher than the FePc molecules of the Kagome lattice, due to a significant lift up of the (t-Bu)$_4$–ZnPc molecules by their *tert*-butyl groups.[43] One of the high-symmetry axes of (t-Bu)$_4$–ZnPc molecule is rotated by ~38° with respect to a lattice vector of the Kagome lattice, similar to that of guest FePc molecules. The structural model of the host–guest supramolecular structures of (t-Bu)$_4$–ZnPc molecules on the Kagome lattice is shown in Figure 2d.

Increasing the coverage of guest FePc molecules to ~0.1 ML (a total coverage of ~0.85 ML that includes a coverage of ~0.75 ML for preparation of the FePc Kagome lattice) results in condensation of the guest molecules into aggregations, instead of random distributed single molecules with higher density, as shown in Figure 3a. Zoom-in images such as the one shown in Figure 3b reveal that all guest FePc molecules are located at the pore sites of the Kagome lattice. Each guest molecule appears as a pear-shaped protrusion, indicating that it adopts a tilted adsorption configuration with one of its lobes partially inserted into a pore of the Kagome lattice.[46] However, the pores of the Kagome lattice around the guest FePc molecules are greatly shrunken, showing a distortion of the Kagome lattice. At a total coverage of ~1 ML, the Kagome

dx.doi.org/10.1021/jp3020244 | J. Phys. Chem. C 2012, 116, 11091–11095

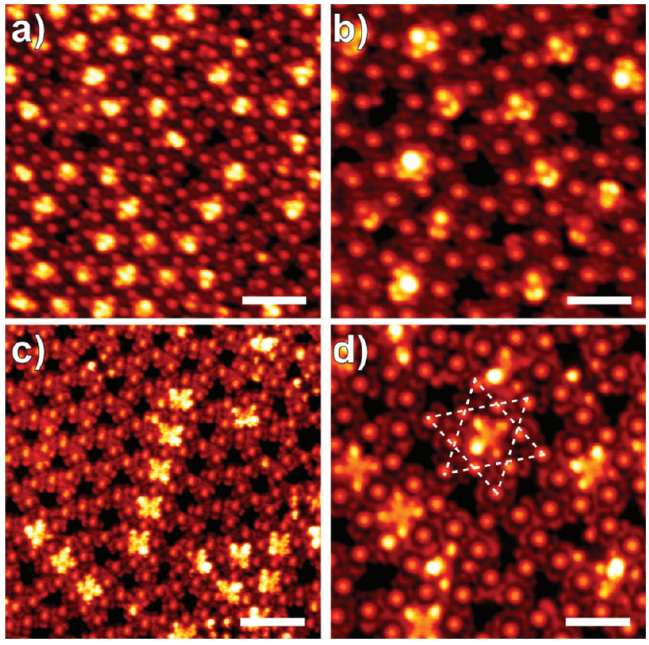

Figure 3. (a and b) STM images of guest FePc molecules on FePc Kagome lattice (scale bar = (a) 5 and (b) 3 nm). (c and d) STM images of guest $(t\text{-Bu})_4$–ZnPc molecules on FePc Kagome lattice (scale bar = (c) 5 and (d) 3 nm). Dashed six-point star in d highlights the Kagome lattice of FePc.

lattice is completely destroyed and the FePc molecules are rearranged into a close-packed square lattice with a lattice parameter of a = 1.05 nm (see Supporting Information). A similar square lattice was also reported for FePc monolayer on Au(111).[46]

In contrast to the case of guest FePc molecules, no significant distortion of the host Kagome lattice is observed after increasing the coverage of guest $(t\text{-Bu})_4$–ZnPc molecules to ~0.08 ML, as illustrated in Figure 3c and 3d. Nevertheless, the guest $(t\text{-Bu})_4$–ZnPc molecules also condense into aggregations (Figure 3c), similar to guest FePc molecules. Each guest $(t\text{-Bu})_4$–ZnPc molecule sits at a pore site of the host Kagome lattice. The guest molecules adopt either a flat adsorption configuration or a tilted one, indicated by the apparent heights of their lobes (Figure 3d). Further increasing the coverage of guest $(t\text{-Bu})_4$–ZnPc molecules to ~0.25 ML leads to an entire occupation of the pores of FePc Kagome lattice. However, the Kagome lattice is greatly distorted and the long-range order is absent for both FePc and $(t\text{-Bu})_4$–ZnPc molecules (see Supporting Information).

Interestingly, a highly ordered host–guest superstructure is formed after coadsorption of guest FePc and $(t\text{-Bu})_4$–ZnPc molecules with a ratio of 1:1 on the Kagome lattice, as depicted in Figure 4a. Survival of the Kagome lattice is clearly seen, despite complete occupation of the pore sites of the Kagome lattice by the guest molecules. The guest molecules showing pear-shaped protrusions are assigned to FePc molecules,[46] whereas those crosses with a dim center and lobes showing nonequivalent apparent heights are attributed to $(t\text{-Bu})_4$–ZnPc molecule.[47] The guest FePc and $(t\text{-Bu})_4$–ZnPc molecule are located at the pore sites of the Kagome lattice and arranged into a highly ordered superstructure with alternate rows. The asymmetrical features that the guest FePc and $(t\text{-Bu})_4$–ZnPc molecules have are evidence that these guest molecules adopt tilted configurations.[46,47] Considering the 3-fold symmetry of

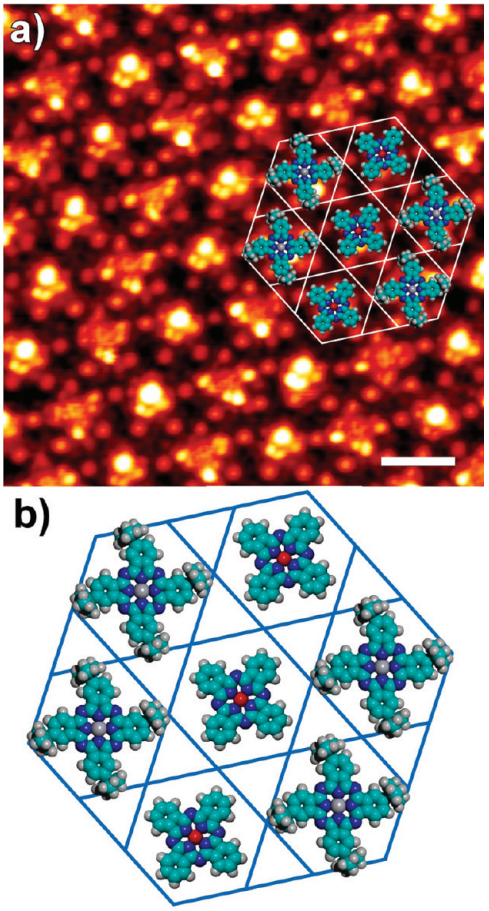

Figure 4. (a) STM image of the highly ordered superstructure with alternate rows of guest FePc and $(t\text{-Bu})_4$–ZnPc molecules on the host Kagome lattice of FePc (scale bar = 3 nm). FePc molecules of the Kagome lattice appear as dim dots constituting a background. Guest FePc and $(t\text{-Bu})_4$–ZnPc molecules are slantingly sitting in the pores of the Kagome lattice, wherein the smaller ones with a brighter center are assigned to FePc molecules, and the larger ones with a darker center are attributed to $(t\text{-Bu})_4$–ZnPc. Structural model is superposed. (b) Structural model of the highly ordered superstructure with alternate rows of guest FePc and $(t\text{-Bu})_4$–ZnPc molecules on the host Kagome lattice of FePc.

the Kagome lattice and the 4-fold symmetry of the guest FePc and $(t\text{-Bu})_4$–ZnPc molecules, three different domains can be distinguished (see Supporting Information). In each domain the same guest species are tilted along an identical direction, whereas different guest species are tilted along different directions. Figure 4b illustrates the structural model of the ordered host–guest complex consisting of alternate FePc and $(t\text{-Bu})_4$–ZnPc molecular rows on the host Kagome lattice.

Formation of surface-supported host–guest complex is essentially governed by the subtle interplay of the host–substrate, guest–substrate, and host–guest interactions. As both FePc and $(t\text{-Bu})_4$–ZnPc molecules prefer to occupying the fcc and hcp regions of the moiré pattern of MG/Ru(0001),[43] preservation of the Kagome lattice of FePc after inclusion of guest FePc and $(t\text{-Bu})_4$–ZnPc molecules at the pores indicates that the interaction between FePc and MG/Ru(0001) is stronger than that between $(t\text{-Bu})_4$–ZnPc and MG/Ru(0001). It is noteworthy that a distorted Kagome lattice with a mixture of FePc and H_2Pc molecules is formed after addition of ~0.05 ML FePc molecules on top of H_2Pc Kagome

dx.doi.org/10.1021/jp3020244 | J. Phys. Chem. C 2012, 116, 11091–11095

lattice (see Supporting Information), suggesting that the interaction between FePc and MG/Ru(0001) is stronger than that between H_2Pc and MG/Ru(0001).

Selective adsorption of the guest FePc and $(t\text{-Bu})_4$–ZnPc molecules at the pore sites of FePc Kagome lattice on MG at low coverage indicates that the interaction between guest and host molecules is not strong enough to attract the guest molecules sitting on top of the host molecules. As the lateral dipole field of MG/Ru(0001) originated from the inhomogeneous charge distribution, which are the dominant driving force for the preferential adsorption of FePc molecules at the fcc and hcp regions,[48] are screened by the FePc Kagome lattice, selective adsorption of the guest molecules at the pore sites of FePc Kagome lattice is guided by the vertical dipole moment at the atop sites of MG/Ru(0001) (the pore site of Kagome lattice). We note that addition of ~0.05 ML C_{60} molecules on the FePc Kagome lattice results in an exclusive location of the C_{60} molecules on top of the FePc molecules instead of at the pore sites of FePc Kagome lattice (see Supporting Information), in contrast to the case of guest FePc and $(t\text{-Bu})_4$–ZnPc molecules on the FePc Kagome lattice.

Formation of a highly ordered superstructure with alternate rows of guest FePc and $(t\text{-Bu})_4$–ZnPc molecules on the host Kagome lattice of FePc evidence a net long-range attractive interaction between guest molecules. Three different mechanisms might count for the unusual long-range interaction between the guest molecules: (1) direct electrostatic and/or van der Waals (vdW) type of interaction between the guest molecules, (2) indirect interactions mediated by the host Kagome lattice due to local conformational modifications,[15,17] and (3) electrostatic interaction through MG. The first mechanism can be ruled out, as the shortest separation of ~3 nm between guest molecules excludes any significant vdW contribution. The second mechanism favors formation of an ordered superstructure of guest molecules by means of conformational mediated indirect coupling between guest molecules via the host Kagome lattice. Once a guest molecule is trapped at a pore site, the conformational structure of the surrounding host FePc molecules is expected to be distorted, which in return will affect the adsorption configuration of neighboring guest molecules. Such host–guest interplay propagates and collectively directs formation of order superstructures with alternate rows of guest FePc and $(t\text{-Bu})_4$–ZnPc molecules on the host FePc Kagome lattice. In fact, the interaction between the host and the guest molecules can result in the pore shrinking of the Kagome lattice around the guest FePc molecules (see Figure 3a and 3b). The distortion of the Kagome lattice and shrinking of the pores will apparently affect the adsorption configuration of the forthcoming guest molecules. A similar mechanism has also been proposed for condensation of C_{60} molecules adsorbed on porphyrin networks.[15,17] The third mechanism should also be considered. As selective adsorption of the guest molecules at the pore sites of FePc Kagome lattice is guided by the vertical dipole moment at the atop sites of MG/Ru(0001), the guest molecules can be polarized by these dipole moments and thus coupled with each other via the dipoles induced by the MG/Ru(0001) substrate. Further experiment and theoretical calculation is under the way in order to clarify the detailed mechanism of the formation of highly ordered superstructure with alternate rows of guest FePc and $(t\text{-Bu})_4$–ZnPc molecules on the host Kagome lattice of FePc.

A variety of host–guest complexes have been fabricated on solid surfaces using either 2D porous networks or organic molecules with cavities.[9,13,15,49–54] However, most of such host–guest complexes are directly adsorbed on metal substrates. Thus, the intrinsic electronic structures of the molecules and the host–guest complexes are inevitably modified due to the coupling between the molecules and the metal substrates. In our present work, efficient decoupling of the molecules from the metal substrates by MG leads to preservation of the intrinsic electronic structures of the molecules,[40–43] making these graphene-based host–guest superstructures ideal model systems for studying the intrinsic properties of host–guest supramolecular complex.

CONCLUSIONS

In summary, we used STM to investigate the accommodation of FePc and $(t\text{-Bu})_4$–ZnPc molecules by the porous Kagome lattices of FePc molecules prepared on MG/Ru(0001). The nanoscale pores of the Kagome lattice of FePc on MG/Ru(0001) exhibit a high affinity to guest FePc and $(t\text{-Bu})_4$–ZnPc molecules. With increasing coverage of guest molecules of either FePc or $(t\text{-Bu})_4$–ZnPc alone, the guest molecules condense into disordered aggregations. Ordered superstructures with alternate rows of FePc and $(t\text{-Bu})_4$–ZnPc are formed after coadsorption of these two species with a ratio of 1:1 onto the Kagome lattice. Condensation of guest molecules and formation of ordered superstructures are controlled by long-range interaction between the guest molecules mediated by the host Kagome lattice with additional contribution from the MG/Ru(0001) substrate. These graphene-based host–guest superstructures might be ideal model systems for studying the intrinsic properties of host–guest supramolecular complexes.

ASSOCIATED CONTENT

Supporting Information

STM images showing the square lattice of FePc at a total coverage of ~1 ML, disordered host–guest complex of $(t\text{-Bu})_4$–ZnPc molecules on FePc Kagome lattice at $(t\text{-Bu})_4$–ZnPc coverage of ~0.25 ML, various domains of host–guest superstructure of FePc and $(t\text{-Bu})_4$–ZnPc molecules on the Kagome lattice of FePc, self-assembly of guest FePc molecules on H_2Pc Kagome lattice, and guest C_{60} molecules on FePc Kagome lattice. This material is available free of charge via the Internet at http://pubs.acs.org.

AUTHOR INFORMATION

Corresponding Author

*E-mail: hjgao@iphy.ac.cn.

Notes

The authors declare no competing financial interest.

ACKNOWLEDGMENTS

Financial support from the NSFC (20973196), National "973" project (2009CB929103, 2010CB923004, and 2011CB932700) of China, and the CAS is gratefully acknowledged.

REFERENCES

(1) Barth, J. V. *Annu. Rev. Phys. Chem.* **2007**, *58*, 375.
(2) Elemans, J. A. A. W.; Lei, S.; De Feyter, S. *Angew. Chem., Int. Ed.* **2009**, *48*, 7298.
(3) Bartel, L. *Nat. Chem.* **2010**, *2*, 87.

(4) Bonifazi, D.; Mohnani, S.; Llanes-Pallask, A. *Chem.—Eur. J.* **2009**, *15*, 7004.
(5) Liang, H.; He, Y.; Ye, Y.; Xu, X.; Cheng, F.; Sun, W.; Shao, X.; Wang, Y.; Li, J.; Wu, K. *Coord. Chem. Rev.* **2009**, *253*, 2959.
(6) Ciesielski, A.; Palma, C.-A.; Bonini, M.; Samori, P. *Adv. Mater.* **2010**, *22*, 3506.
(7) Slater, A. G.; Beton, P. H.; Champness, N. R. *Chem. Sci.* **2011**, *2*, 1440.
(8) Otsuki, J. *Coord. Chem. Rev.* **2010**, *254*, 2311.
(9) Theobald, J. A.; Oxtoby, N. S.; Phillips, M. A.; Champness, N. R.; Beton, P. H. *Nature* **2003**, *424*, 1029.
(10) Pawin, G.; Wong, K. L.; Kwon, K.-Y.; Bartels, L. *Science* **2006**, *313*, 961.
(11) Blunt, M. O.; Russell, J. C.; del Carmen Giménez-López, M.; Garrahan, J. P.; Lin, X.; Schröder, M.; Champness, N. L.; Beton, P. H. *Science* **2008**, *322*, 1077.
(12) Xiao, W. D.; Feng, X. L.; Ruffieux, P.; Gröning, O.; Műllen, K.; Fasel, R. *J. Am. Chem. Soc.* **2008**, *130*, 8910.
(13) Stepanow, S.; Lingenfelder, M.; Dmitriev, A.; Spillmann, H.; Delvigne, E.; Lin, N.; Deng, X.; Cai, C.; Barth, J. V.; Kern, K. *Nat. Mater.* **2004**, *3*, 229.
(14) Berner, S.; de Wild, M.; Ramoino, L.; Ivan, S.; Baratoff, A.; Gűnterodt, H.-J.; Suzuki, H.; Schlettwein, D.; Jung, T. A. *ChemPhysChem* **2001**, *68*, 115410.
(15) Bonifazi, D.; Spillmann, H.; Kiebele, A.; de Wild, M.; Seiler, P.; Cheng, F.; Güntherodt, H.; Jung, T.; Diederich, F. *Angew. Chem., Int. Ed.* **2004**, *43*, 4759.
(16) Griessl, S. J. H.; Lackinger, M.; Jamitzky, J.; Markert, T.; Hietschold, M.; Heckl, W. M. *J. Phys. Chem. B* **2004**, *108*, 11556.
(17) Spillmann, H.; Kiebele, A.; Stöhr, M.; Jung, T. A.; Bonifazi, D.; Cheng, F.; Diederich, F. *Adv. Mater.* **2006**, *18*, 279.
(18) Schull, G.; Douillard, L.; Fiorini-Debuisschert, C.; Charra, F.; Mathevet, F.; Kreher, D.; Attias, A. J. *Adv. Mater.* **2006**, *18*, 2954.
(19) Li, M.; Deng, Q.-D.; Lei, S.-B.; Yang, Y.-L.; Wang, T.-S.; Chen, Y.-T.; Wang, C.-R.; Zeng, Q.-D.; Wang, C. *Angew. Chem., Int. Ed.* **2008**, *47*, 6717.
(20) Tahara, K.; Lei, S.; Mamdouh, W.; Yamaguchi, Y.; Ichikawa, T.; Uji-I, H.; Sonoda, M.; Hirose, K.; De Schryver, F. C.; De Feyter, S.; Tobe, Y. *J. Am. Chem. Soc.* **2008**, *130*, 6666.
(21) Madueno, R.; Räisänen, M. T.; Silien, C.; Buck, M. *Nature* **2008**, *454*, 618.
(22) Blunt, M. O.; Russell, J. C.; Gimenez-Lopez, M. C.; Taleb, N.; Lin, X.; Schröder, M.; Champness, N. R.; Beton, P. H. *Nat. Chem.* **2011**, *3*, 74.
(23) Wei, Y.; Reutt-Robey, J. E. *J. Am. Chem. Soc.* **2011**, *133*, 15232.
(24) MacLeod, J. M.; Ivasenko, O.; Fu, C.; Taerum, T.; Rosei, F.; Perepichka, D. F. *J. Am. Chem. Soc.* **2009**, *131*, 16844.
(25) Wei, Y.; Robey, S. W.; Reutt-Robey, J. E. *J. Am. Chem. Soc.* **2009**, *131*, 12026.
(26) Castro Neto, A. H.; Guinea, F.; Peres, N. M. R.; Novoselov, K. S.; Geim, A. K. *Rev. Mod. Phys.* **2009**, *81*, 109.
(27) Das Sarma, S.; Adam, S.; Hwang, E. H.; Rossi, E. *Rev. Mod. Phys.* **2011**, *83*, 407.
(28) Wu, Y. H.; Yu, T.; Shen, Z. X. *J. Appl. Phys.* **2010**, *108*, 071301.
(29) Bostwick, A.; McChesney, J.; Ohta, T.; Rotenberg, E.; Seyller, T.; Horn, K. *Prog. Surf. Sci.* **2009**, *84*, 380.
(30) Pan, Y.; Shi, D. X.; Gao, H.-J. *Chin. Phys.* **2007**, *16*, 3151.
(31) Sutter, P. W.; Flege, J. I.; Sutter, E. A. *Nat. Mater.* **2008**, *7*, 406.
(32) Marchini, S.; Gunther, S.; Wintterlin, J. *Phys. Rev. B* **2007**, *76*, 075429.
(33) Pan, Y.; Zhang, H.; Shi, D.; Sun, J.; Du, S.; Liu, F.; Gao, H.-J. *Adv. Mater.* **2009**, *21*, 2777.
(34) N'Diaye, A. T.; Bleikamp, S.; Feibelman, P. J.; Michely, T. *Phys. Rev. Lett.* **2006**, *97*, 215501.
(35) Ueta, H.; Saida, M.; Nakai, C.; Yamada, Y.; Sasaki, M.; Yamamoto, S. *Surf. Sci.* **2004**, *560*, 183.
(36) Gao, M.; Pan, Y.; Zhang, C. D.; Hu, H.; Yang, R.; Lu, H. L.; Cai, J. M.; Du, S. X.; Liu, F.; Gao, H.-J. *Appl. Phys. Lett.* **2010**, *96*, 053109.
(37) Varykhalov, A.; Sanchez-Barriga, J.; Shikin, A. M.; Biswas, C.; Vescovo, E.; Rybkin, A.; Marchenko, D.; Rader, O. *Phys. Rev. Lett.* **2008**, *101*, 157601.
(38) Dedkov, Y. S.; Fonin, M.; Rudiger, U.; Laubschat, C. *Phys. Rev. Lett.* **2008**, *100*, 107602.
(39) Gao, L.; Guest, J. R.; Guisinger, N. P. *Nano Lett.* **2010**, *10*, 3512.
(40) Barja, S.; Garnica, M.; Hinarejos, J. J.; de Parga, A. L. V.; Martin, N.; Miranda, R. *Chem. Commun.* **2010**, *46*, 8198.
(41) Zhou, H. T.; Mao., J. H.; Li, G.; Wang, Y. L.; Feng, X. L.; Du, S. X.; Műllen, K.; Gao, H.-J. *Appl. Phys. Lett.* **2011**, *99*, 153101.
(42) Dou, W.; Huang, S.; Zhang, R. Q.; Lee, C. S. *J. Chem. Phys.* **2011**, *134*, 094705.
(43) Mao, J. H.; Zhang, H. G.; Jiang, Y. H.; Pan, Y.; Gao, M.; Xiao, W. D.; Gao, H.- J. *J. Am. Chem. Soc.* **2009**, *131*, 14136.
(44) Syôzi, I. *Prog. Theor. Phys.* **1951**, *6*, 306.
(45) Lu, X.; Hipps, K. W. *J. Phys. Chem. B* **1997**, *101*, 5391.
(46) Cheng, Z. H.; Gao, L.; Deng, Z. T.; Liu, Q.; Jiang, N.; Lin, X.; He, X. B.; Du, S. X.; Gao, H.-J. *J. Phys. Chem. C* **2007**, *111*, 2656.
(47) Cheng, Z. H.; Du, S. X.; Jiang, N.; Zhang, Y. Y.; Guo, W.; Hofer, W. A.; Gao, H.-J. *Surf. Sci.* **2011**, *605*, 415.
(48) Zhang, H. G.; Sun, J. T.; Low, T.; Zhang, L. Z.; Pan, Y.; Liu, Q.; Mao, J. H.; Zhou, H. T.; Guo, H. M.; Du, S. X.; Guinea, F.; Gao, H.-J. *Phys. Rev. B* **2011**, *84*, 245436.
(49) Pan, G.; Liu, J.; Zhang, H.; Wan, L.; Zheng, Q.; Bai, C. *Angew. Chem., Int. Ed.* **2003**, *42*, 2747.
(50) Mena-Osteritz, E.; Bäuerle, P. *Adv. Mater.* **2006**, *18*, 447.
(51) Xiao, W. D.; Passerone, D.; Ruffieux, P.; Aït-Mansour, K.; Gröning, O.; Tosatti, E.; Siegel, J.; Fasel, R. *J. Am. Chem. Soc.* **2008**, *130*, 4767.
(52) Huang, Y. L.; Chen, W.; Li, H.; Ma, J.; Pfaum, J.; Wee, A. T. S. *Small* **2010**, *6*, 70.
(53) Hipps, K. W.; Scudiero, L.; Barlow, D. E.; Cooke, M. P., Jr. *J. Am. Chem. Soc.* **2002**, *124*, 2126.
(54) Calmettes, B.; Nagarajan, S.; Gourdon, A.; Abel, M.; Porte, L.; Coratger, R. *Angew. Chem., Int. Ed.* **2008**, *47*, 6994.